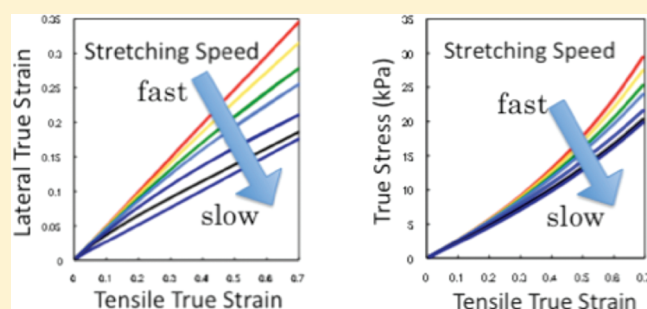


# Strain-Rate-Dependent Poisson's Ratio and Stress of Polymer Gels in Solvents Revealed by Ultraslow Stretching

Akihiro Konda, Kenji Urayama,\* and Toshikazu Takigawa

Department of Materials Chemistry, Kyoto University, Nishikyo-ku, Kyoto 615-8510, Japan

**ABSTRACT:** Pronounced strain-rate-dependent Poisson's ratio ( $\mu$ ) and stress ( $\sigma$ ) are observed for a fully swollen gel (60 mm in length and 1.2 mm in thickness) in solvents when greatly stretched in tensile experiments with a wide range of crosshead speeds ( $v$ ), across 5 orders of magnitude from an extremely slow  $v$  of 0.17  $\mu\text{m/s}$ . The strain-rate dependence is the result of the stretching-driven swelling during deformation and not viscoelastic effects. This feature is unique to polymer gels that behave as semiopen systems, i.e., systems that can exchange solvent with its surroundings. When  $v$  is so low that the time scale of stretching ( $\dot{\epsilon}_0^{-1}$  where  $\dot{\epsilon}_0 = v/l_0$  is the initial strain rate and  $l_0$  the initial length) is comparable to the characteristic time of swelling ( $\tau$ ),  $\mu$  and  $\sigma$  become strongly dependent on  $v$ :  $\mu$  becomes less than 1/2 and  $\sigma$  becomes smaller than the value corresponding to the sufficiently high  $v$  (satisfying the relation  $\dot{\epsilon}_{0-1} \ll \tau$ ) where no volume change occurs ( $\mu = 1/2$ ). In the low  $v$  limit ( $\dot{\epsilon}_{0-1} \gg \tau$ ), the strain-induced swelling is equilibrated at all times during stretching:  $\mu$  ( $\approx 0.25$ ) and  $\sigma$  are at equilibrium values, independent of  $v$ . A model to describe the  $v$  dependence of  $\mu$  and stress–strain relation is developed from the existing model for swelling dynamics under a small step strain on the basis of the Boltzmann superposition principle. The model well captures the main features of the experimental results. The results of the present study also provide fundamental information about the effects that the actuation rate has on the mechanical performance of gel-based soft actuators because this effect becomes pronounced at easily attainable deformation speeds for microfabricated gels and fiber gels with relatively short characteristic time for swelling.



## INTRODUCTION

Polymer gels vary their volume in response to the change in environmental parameters such as temperature, solvent composition, etc.<sup>1</sup> This stimulus-responsive swelling behavior of polymer gels opens the way for potential applications in drug delivery and the development of soft actuators. An externally imposed strain (or stress) may also lead to changes in the volume of polymer gels,<sup>2–11</sup> but significant less attention has been paid to this phenomenon as compared to other stimuli such as variations in the surrounding temperature and solvent composition. Further swelling<sup>3,4,9,10</sup> (or shrinking<sup>2,5,6,11</sup>) occurs when fully swollen gels undergo constant uniaxial stretching (or compression) in solvents. At the same time, the induced swelling (or shrinking) is the source of a considerable reduction observed in the tensile (or compressive) force originally exerted.<sup>3,4,11</sup> Importantly, the major cause of this stress relaxation is not viscoelastic effects but the decrease in the effective strain for the stress due to volume change. This is evident from the fact that (1) the characteristic time of stress reduction ( $\tau_\sigma$ ) is similar to that of strain-induced swelling ( $\tau_{sw}$ ) and (2) in contrast to the viscoelastic relaxation time  $\tau_\sigma$  is proportional to the square of the gel dimensions.<sup>4</sup> The simultaneous strain-induced swelling and stress reduction observed under constant strain imply that the stress–strain relation of polymer gels deformed in solvents depends to a great extent on the strain rate. Strain-rate-dependent

stress of this type, which is not the result of viscoelastic effects, is characteristic of polymer gels that are semiopen systems, i.e., can exchange solvent with its surroundings. However, such strain-rate-dependent stress is hardly observed in conventional tensile experiments because that would require an unrealistically slow strain rate for a gel with dimensions of the order of centimeters and millimeters. More specifically, for a gel with a length ( $l$ ) of 10 mm and a thickness ( $a$ ) of 1 mm, the corresponding crosshead speed ( $v_c$ ) is estimated to be approximately equal to  $v_c \approx l/\tau_{sw} \approx lD/a^2 \approx 1 \mu\text{m/s}$ , where  $D$  is the diffusion constant of polymer networks, typically equal to  $D \approx 10^{-10} \text{ m}^2/\text{s}$ . As is evident from the definition, the necessary  $v_c$  is easily attainable for gels of relatively small dimensions or thin gel films:  $v_c \approx 0.1 \text{ mm/s}$  for a gel film with  $l = 10 \text{ mm}$  and  $a = 100 \mu\text{m}$ . In other words, the stress developed in gels of such small dimensions or thin gel films is considerably dependent on the strain rate. The strain-rate-dependent stress is an important factor that needs to be considered when actuating microfabricated gels or fiber gels because it significantly affects their mechanical performance.

**Received:** December 7, 2010

**Revised:** February 1, 2011

**Published:** March 16, 2011

In a previous study,<sup>9</sup> we observed variations in the dimensions of a fully swollen fine gel ( $l = 20$  mm and  $a = 400$   $\mu\text{m}$ ) subjected in water to a sinusoidal oscillating force with varying angular frequency ( $\omega$ ). The gel exhibited a pronounced  $\omega$  dependence of the Poisson's ratio ( $\mu$ ), defined by the ratio of the strain amplitudes in the directions parallel and normal to exerted tensile force. The onset frequency for the variation of  $\mu$  ( $\omega_c$ ) was found to be correlated with  $\tau_{\text{sw}}$  and more precisely,  $\omega_c \approx \tau_{\text{sw}}^{-1}$ . During these force-controlled measurements, the strain of interest was very small as within the linear elasticity regime, and no information about the  $\omega$  dependence on stress or the effects of a very large strain on the induced swelling of the gel could be obtained.

In this study, we have conducted a series of tensile straining experiments where a hydrogel was stretched in water over a wide range of crosshead speeds ( $8.3 \times 10^3$   $\mu\text{m/s} > v > 0.17$   $\mu\text{m/s}$ ) up to a high strain of 100%. The range of  $v$  is sufficiently wide to cover two extreme cases, i.e., the deformation of the gel without volume change ( $\mu = 1/2$ ) and with full volume change caused by the strain-induced swelling at all times during the stretching process. A 1 mm thick gel is employed as a sample because a precise measurement of tensile force was relatively difficult for gels of a smaller thickness and cross section. Furthermore,  $v_c$  is so low for a 1 mm thick gel that it cannot be attained by means of a conventional tensile tester. We employed, therefore, a custom-made tensile tester to achieve extremely slow stretching of  $v < 1$   $\mu\text{m/s}$ . We were able to reveal the whole aspects of the  $v$  effect on the nonlinear stress–strain behavior of the gels stretched in solvents. To describe the experimental results, we developed a theoretical model based on existing models of the swelling behavior observed after the application of a relatively small step strain. Lastly, the results of the present study provide fundamental information about the effects that the actuation rate has on the mechanical performance of gel-based soft actuators.

## THEORY OF THERMODYNAMICS AND KINETICS OF STRETCHING-DRIVEN SWELLING

**Thermodynamics.** In this section, we briefly describe the theoretical background of the thermodynamics of stretching-driven swelling of gels on the basis of the classical Flory–Rehner theory.<sup>12</sup> First, we consider the effects of a stretch of  $\alpha_x$  imposed on a rectangular gel that is fully swollen in solvents and characterized by a network volume fraction of  $\phi_0$  (Figure 1). The free energy change ( $\Delta F$ ) upon swelling is given by a sum of the contributions of isotropic mixing ( $\Delta F_{\text{mix}}$ ) between the network and solvent and the deformation of networks by rubber elasticity ( $\Delta F_{\text{el}}$ ). The Flory–Huggins lattice model and classical rubber elasticity theory provide the expressions of  $\Delta F_{\text{mix}}$  and  $\Delta F_{\text{el}}$ , respectively:<sup>13</sup>

$$\begin{aligned} \Delta F/k_B T &= (\Delta F_{\text{mix}} + \Delta F_{\text{el}})/k_B T \\ &= N_s [\ln(1 - \phi) + \chi \phi] + N_c (\lambda_x^2 + \lambda_y^2 + \lambda_z^2 - 3)/2 \end{aligned} \quad (1)$$

where  $k_B$  is the Boltzmann constant,  $T$  the absolute temperature,  $N_s$  the number of solvent molecules,  $N_c$  the number of elastically effective network chains, and  $\chi$  the Flory–Huggins solubility parameter. The principal ratio  $\lambda_i$  ( $i = x, y, z$ ) represents the deformation measured at a reference state, while  $\lambda_i$  is expressed as  $\lambda_i = \lambda_s \alpha_i$ , where  $\lambda_s (= \phi_0^{-1/3})$  is the isotropic expansion due to free swelling. The gel network volume fraction  $\phi$  is defined as a

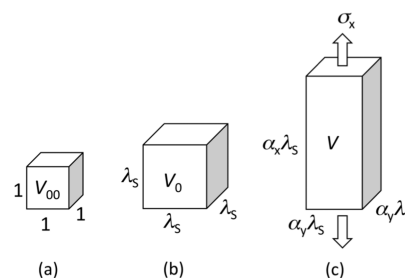


**Figure 1.** Schematic diagram of the stretching-driven swelling of polymer gels: (a) reference (dry) state; (b) fully swollen state when no stress is exerted; (c) swollen state after imposing a stretch of  $\alpha_x$ .

function of  $\lambda_i$  and  $\alpha_i$  ( $i = x, y, z$ ) according to the expression  $\phi^{-1} = V/V_{00} = \lambda_x \lambda_y \lambda_z$  and  $\phi_0/\phi = \alpha_x \alpha_y \alpha_z$ , where  $V$  and  $V_{00}$  are the volume of the gel in the swollen and reference state, respectively. The true stress (force per cross section in the deformed state)  $\sigma_i$  ( $i, j, k = x, y, z$ ) is given by the following equation:

$$\sigma_i = \frac{1}{l_i l_k} \left( \frac{\partial \Delta F}{\partial l_i} \right) = \frac{1}{V_{00} \lambda_j \lambda_k} \left( \frac{\partial \Delta F}{\partial \lambda_i} \right) \quad (2)$$

where  $l_i$  is the dimension along the  $i$ -direction in the deformed state. The following relation is obtained from the condition that the stresses in the  $y$ - and  $z$ -directions are zero at equilibrium under stretching, i.e.,  $\sigma_y = \sigma_z = 0$  at  $\lambda_x = \lambda_0 \alpha_x$ :

$$\begin{aligned} \sigma_y = \sigma_z &= \frac{N_s k_B T}{(1 - \phi)V} [\ln(1 - \phi) + \phi + \chi \phi^2] + \frac{N_c \phi_0^{1/3} k_B T}{V_{00} \alpha_x} \\ &= 0 \end{aligned} \quad (3)$$

Equation 3 is also satisfied before stretching ( $\alpha_x = 1$  and  $\phi = \phi_0$ ). On the basis of these equations, the following relation is obtained for highly swollen gels with  $\phi \ll 1$  and  $\phi_0 \ll 1$ :

$$\alpha_y = \alpha_x^{-1/4} \quad (4)$$

where the approximation  $\ln(1 - \phi) \approx -\phi - \phi^2/2$  is used. The exponent in eq 4 corresponds to Poisson's ratio ( $\mu$ ):

$$\mu = -\varepsilon_y/\varepsilon_x = -\ln \alpha_y/\ln \alpha_x \quad (5)$$

where  $\varepsilon_i$  is the true strain in the  $i$ -direction ( $\varepsilon_i = \ln \alpha_i$ ). Equation 5 is a generalized definition of  $\mu$  whose validity is extended to any finite strain; namely, it is not limited to relatively small strains. From eq 4, the equilibrium (osmotic) Poisson's ratio ( $\mu_\infty$ ) for highly swollen gels is

$$\mu_\infty = 1/4 \quad (6)$$

independently of  $\alpha_x$ . Poisson's ratio is a measure of the strain-induced volume change, which is evident from the relation  $V/V_0 = \alpha_x^{1-2\mu}$ . A value of  $\mu$  less than 1/2 means that the stretching ( $\alpha_x > 1$ ) drives further swelling of the gel ( $V > V_0$ ). It should be noticed that further lateral swelling results in an increase in configurational entropy of the stretched networks (in other words, it leads to a decrease in the anisotropy of the stretched networks). This qualitatively explains the physical origin of stretching induced swelling. The same value of  $\mu_\infty$  for highly swollen gels under high stretching was derived by several authors using a blob model by several authors.<sup>14,15</sup> For highly swollen gels subjected to infinitesimal deformation ( $\alpha_x \approx 1$ ), the similar values of  $\mu_\infty$

(1/6 and 0.278) were obtained by using eq 1 but with a logarithmic term in the early Flory theory<sup>4</sup> and a scaling approach for good solvent systems,<sup>16</sup> respectively.

The true stress  $\sigma_x$  is obtained from eqs 2 and 3:

$$\begin{aligned}\sigma_x &= \nu_c k_B T \phi_0^{1/3} (\alpha_x^{2\mu+1} - \alpha_x^{-1}) \\ &= G(\alpha_x^{2\mu+1} - \alpha_x^{-1})\end{aligned}\quad (7)$$

where  $\alpha_y = \alpha_x^{-\mu}$  is used, and  $G$  is the shear modulus at  $\phi = \phi_0$  given by  $G = \nu_c k_B T \phi_0^{1/3}$ . The equilibrium stress ( $\sigma_\infty$ ) is given by eq 7 with  $\mu_\infty = 1/4$  as

$$\sigma_\infty = G(\alpha_x^{3/2} - \alpha_x^{-1}) \quad (8)$$

Equation 7 with  $\mu = 1/2$  gives the familiar stress–strain relation in the case where there is no volume change, which is derived from classical rubber elasticity theory:<sup>17</sup>

$$\sigma_0 = G(\alpha_x^2 - \alpha_x^{-1}) \quad (9)$$

The relation  $\sigma_0 > \sigma_\infty$  for each  $\alpha_x$  indicates that the strain-induced swelling after the imposition of a step constant strain results in a stress reduction. It should be emphasized that this stress reduction is not entirely attributed to an increase in the cross section of the gel caused by strain-induced swelling. This is more pronounced in the nominal stress  $\sigma^n$  ( $\sigma^n = \sigma \alpha_x^{-2\mu}$ ; force per cross section at the undeformed state). The nominal stress corresponding to  $\sigma_\infty$  and  $\sigma_0$  are given by  $\sigma_\infty^n = G(\alpha_x - \alpha_x^{-3/2})$  and  $\sigma_0^n = G(\alpha_x - \alpha_x^{-2})$ , respectively. The relation  $\sigma_0^n > \sigma_\infty^n$  for each  $\alpha_x$  shows that the strain-induced swelling reduces the tensile force. This behavior is attributed to a reduction in the effective tensile strain exerted on the gel: the strain-induced swelling of the gel results in a volume increase from  $V_0$  to  $V$ , and at the stress-free state, the length of the gel with  $V$  is larger than that with  $V_0$ . Lastly, we mention about the initial (small-strain) Young's modulus  $E(\phi)$  in the induced swollen state ( $\sigma_x = E \varepsilon_x$ ). The modulus  $E(\phi)$  is expressed by  $E(\phi) = 2(\mu + 1)G$ , where  $\mu$  is the Poisson's ratio at the corresponding  $\phi$ , which is obtained from the linear elasticity theory and can also be derived from eq 7 with  $\alpha_x \approx 1 + \varepsilon_x$ . It is found that the induced swelling changes  $E$  from  $3G$  to  $5G/2$  as a result of the variation in  $\mu$  from  $\mu_0 = 1/2$  to  $\mu_\infty = 1/4$ .

**Kinetics.** We subsequently consider the variations in the lateral dimension and a tensile stress exerted on the gel while this is being stretched at a constant strain rate ( $\dot{\varepsilon}$ ). The basis of this analysis is in the swelling dynamics after a step constant strain, which has been theoretically demonstrated in the past by several authors.<sup>3,4,18,19</sup> Doi et al.<sup>18,19</sup> proposed a rigorous model considering the solvent motion during swelling, while earlier studies<sup>3,4</sup> assumed a quiescent solvent. As these two approaches result in no pronounced difference in the kinetics results,<sup>18–20</sup> we employ here the first model for the sake of mathematical simplicity. The swelling of the gel can be decomposed into longitudinal and transverse diffusion modes, which govern the volume change and the shape change without volume change, respectively.<sup>4</sup> The phenomena of interest to our study is governed by the longitudinal mode. Specifically, the swelling of a rectangular gel subjected to a tensile strain of  $\varepsilon_x$  can be assumed to occur in  $y$ - and  $z$ -direction. In this case, the volume change is given by the change of the cross-sectional area on the  $yz$  plane, i.e.,  $\text{Tr}(\mathbf{u}) = u_{yy} + u_{zz}$ , where  $\mathbf{u}$  is the strain tensor of small volume element and  $\text{Tr}$  is the trace in a two-dimensional space. The time dependence of  $\text{Tr}(\mathbf{u})$  obeys the diffusion equation defined in

two-dimensional space as<sup>4</sup>

$$\frac{\partial}{\partial t} \text{Tr}(u_{ij}) = D_L \nabla^2 \text{Tr}(u_{ij}) \quad (10)$$

where  $D_L$  is identical to the collective diffusion constant introduced by Tanaka et al.<sup>21</sup> The diffusion constant  $D_L$  is given by  $D_L = (K_{os} + 4G/3)/\zeta$ , where  $K_{os}$  and  $\zeta$  are the osmotic bulk modulus and the friction coefficient between network and solvent, respectively. The initial and boundary conditions for eq 10 are

$$\text{Tr}(u_{ij}) = \varepsilon_{y0} + \varepsilon_{z0} = -2\mu_0 \varepsilon_x \quad \text{at } t = 0 \quad (11)$$

$$\text{Tr}(u_{ij}) = \varepsilon_{y\infty} + \varepsilon_{z\infty} = -2\mu_\infty \varepsilon_x \quad \text{at boundaries} \quad (11b)$$

where  $\varepsilon_{i0}$  and  $\varepsilon_{i\infty}$  ( $i = y, z$ ) are the macroscopic strains in the initial and equilibrium states, respectively. The solution of eq 10 satisfying eq 11 is

$$\text{Tr}(u_{ij}) = -2\mu(y, z, t) \varepsilon_x \quad (12a)$$

where

$$\begin{aligned}\mu(y, z, t) &= \\ \mu_\infty + \sum_{m,n}^{\text{odd}} \frac{16(\mu_0 - \mu_\infty)}{mn\pi^2} \sin \frac{m\pi y}{a_r} \sin \frac{n\pi z}{a_r} \exp \left[ -\frac{(m^2 + n^2)t}{2\tau_1} \right]\end{aligned}\quad (12b)$$

The quantity  $a_r$  is the dimension of the gel in the  $y$ - and  $z$ -directions in the reference state, and  $\tau_1$  is the longest characteristic time given by  $\tau_1 = a_r^2 / (2\pi^2 D_L)$ . As the surface of the rectangular gel during the swelling process has a convex profile in the  $yz$  plane, the macroscopic strain  $\varepsilon_y$  ( $=\varepsilon_z$ ) for a rectangular gel after small elongation is given by averaging  $\text{Tr}(u_{ij})$ :

$$\varepsilon_y(t) = \frac{1}{2a_r^2} \int_0^{a_r} \int_0^{a_r} dy dz \text{Tr}(u_{ij}) \quad (13)$$

When the gel is stretched in the  $x$ -direction at a strain rate of  $\dot{\varepsilon}$ ,  $\varepsilon_x(t)$  is expressed by

$$\varepsilon_x(t) = \int_0^t \dot{\varepsilon} dt' \quad (14)$$

The corresponding finite lateral strain  $\varepsilon_y(t)$  for the elongation process can be written by developing eqs 12 and 13 on the basis of the Boltzmann superposition principle:<sup>22</sup>

$$\varepsilon_y(t) = \int_0^t m(t-t') \dot{\varepsilon} dt' \quad (15a)$$

where the response function  $m(t-t')$  is given by

$$\begin{aligned}m(t-t') &= -\frac{1}{a_r^2} \int_0^{a_r} \int_0^{a_r} \mu(y, z, t-t') dy dz \\ &= -\mu_\infty - \sum_{m,n}^{\text{odd}} \frac{64(\mu_0 - \mu_\infty)}{m^2 n^2 \pi^4} \exp \left[ -\frac{(m^2 + n^2)(t-t')}{2\tau_1} \right]\end{aligned}\quad (15b)$$

In the experiments, the gel underwent stretching at a constant crosshead speed ( $v$ ). It should be noted that in this case the strain rate becomes smaller with stretching (or time), and  $\dot{\varepsilon}$  in eqs 14

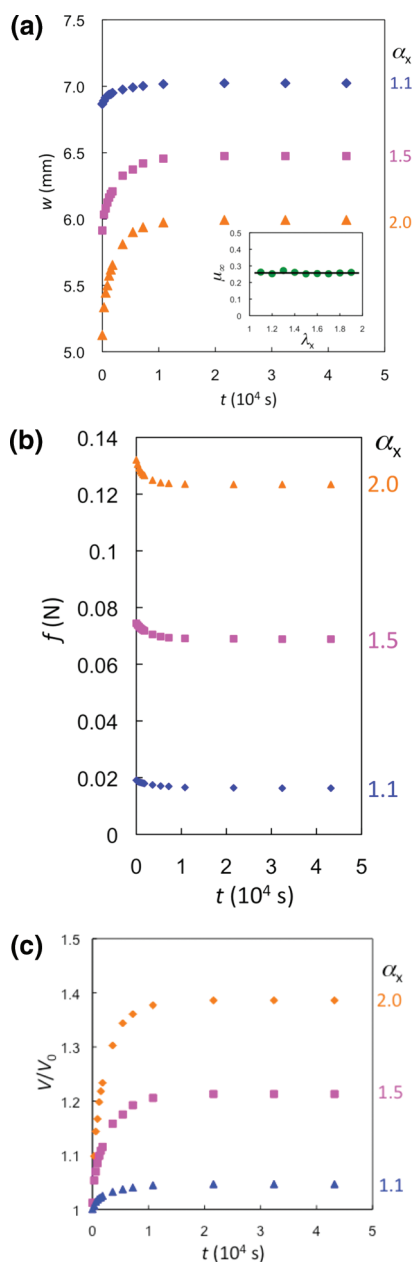


**Figure 2.** Swelling and force reduction of a poly(acrylamide) hydrogel in water under constant elongation. (a) Gel width ( $w$ ), (b) tensile force ( $f$ ), and (c) volume ratio ( $V/V_0$ ) as a function of the time that has elapsed since a constant stretch of  $\alpha_x = 1.1$ ,  $1.5$ , and  $2.0$  was imposed on the sample gel. The inset in (a) shows the  $\alpha_x$  dependence of the equilibrium Poisson's ratio ( $\mu_\infty$ ).

and 15 is replaced by

$$\dot{\epsilon}(t) = \frac{\dot{\epsilon}_0}{1 + \dot{\epsilon}_0 t} = \frac{v}{l_0 + vt} \quad (16)$$

where  $\dot{\epsilon}_0$  is the initial strain rate given by  $\dot{\epsilon}_0 = v/l_0$  for the initial length of  $l_0$ .

## EXPERIMENTAL SECTION

**Sample Preparation.** Poly(acrylamide) gels were prepared by radical copolymerization of an acrylamide monomer and methylenebis(acrylamide) (cross-linker). Ammonium persulfate was used as initiator of polymerization.

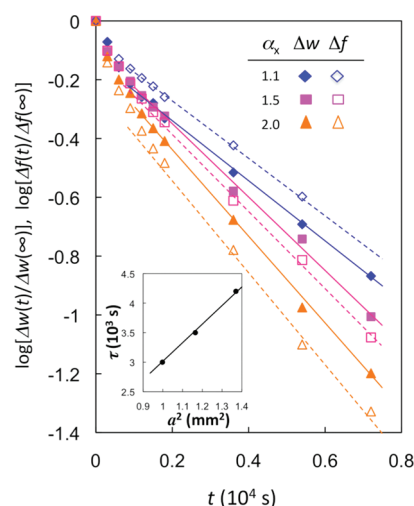


**Figure 3.** Semilog plots of  $\Delta w(t)/\Delta w(\infty)$  and  $\Delta f(t)/\Delta f(\infty)$  versus time where  $\Delta w(t) = w(0) - w(t)$  and  $\Delta f(t) = f(0) - f(t)$  were estimated based on experimental data shown in Figure 2. The inset shows the dependence of the longest characteristic time ( $\tau_1$ ), which is estimated as the inverse of the slope of each curve, on the square of the equilibrium thickness ( $a^2$ ) for each stretched state.

The mixture was dissolved in water. The total reactant concentration was 10 wt %, and the molar ratio [monomer]/[cross-linker] was 200. Gelation was conducted at 5 °C for 24 h in a glass mold. The resultant rectangular gel was left to swell in water until an equilibrium was achieved. The polymer concentration was 6.2 wt % at the fully swollen state where the unreacted materials were washed out. For the tensile experiments, we employed the fully swollen hydrogel of  $60 \times 7.2 \times 1.2$  mm.

**Tensile Measurements.** The tensile measurements were conducted using a UTM-4-100 (Toyo Baldwin Co., Japan) at a constant crosshead speed ( $v$ ). The apparatus was modified so that stretching at an extremely low speed of  $0.17 \mu\text{m/s}$  could be possible. RTM-250 (Orientec, Japan) was employed for the fast tensile measurements at a crosshead speed of  $v > 1 \text{ mm/s}$ . The crosshead speeds were varied in the wide range from  $0.17$  to  $8300 \mu\text{m/s}$ , namely, 5 orders of magnitude. The fully swollen hydrogel was stretched in a transparent glass bath filled with water at 25 °C. The variations in the lateral dimension were observed during the stretching process by means of a CCD camera, and the lateral strain was evaluated through video analysis techniques. The experimental error in the measurement of gel dimension was estimated to be  $\pm 5 \mu\text{m}$ . The dependence of tensile force and lateral strain on imposed stretching was investigated at various values of  $v$ . At each  $v$ , the specimen was stretched to  $\alpha_x = 2$  ( $\epsilon_x \approx 0.69$ ). The stretching to  $\alpha_x = 2$  required  $\sim 7 \text{ s}$  or  $4 \times 10^5 \text{ s}$  (i.e.,  $\sim 5$  days) for the highest or lowest value of  $v$ , respectively. After the stretching to  $\alpha_x = 2$ , the imposed strain was fully released. The specimen was stretched again at different  $v$  after equilibrating the swelling in the stress-free state. The interval between successive tensile measurements was 1 day.

The strain-induced swelling and stress reduction observed after the application of a step strain was also investigated. The gel was elongated at a crosshead speed of  $v = 8300 \mu\text{m/s}$  to the destination  $\alpha_x$ , and the time dependence of lateral dimension and stress under the constant  $\alpha_x$  was examined.

## RESULTS AND DISCUSSION

**Swelling and Stress Reduction under Constant Stretching.** Figure 2a,b shows the lateral dimension ( $w$ ) and tensile force ( $f$ ) as a function of time for the gel under constant stretching of  $\alpha_x = 1.1$ ,



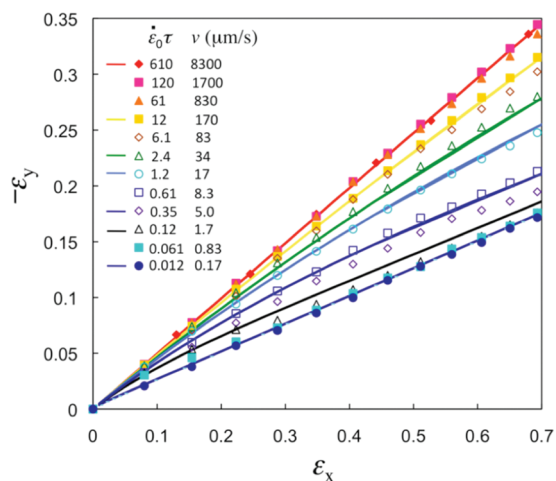


**Figure 4.** Relation between imposed true strain ( $\varepsilon_x$ ) and lateral true strain ( $\varepsilon_y$ ) for a poly(acrylamide) hydrogel undergoing stretching in water over a wide range of crosshead speeds ( $v$ ). The solid lines represent theoretical predictions.

1.5, or 2.0. In these figures,  $t = 0$  is the point in time when the elongation reached the destination  $\alpha_x$ . Stretching-induced swelling is observed at every value of  $\alpha_x$ ; i.e.,  $w$  increases slowly with time and reaches the equilibrium. Simultaneously,  $f$  decreases gradually and finally reaches the equilibrium value. The inset of Figure 2a displays the  $\alpha_x$  dependence of the equilibrium Poisson's ratio ( $\mu_\infty$ ) estimated from eq 5 with the equilibrium value of  $\varepsilon_y$ . The ratio  $\mu_\infty$  is  $\sim 0.25$  and independent of  $\alpha_x$ , which is in good agreement with theoretical predictions for highly swollen gels (eq 6). Figure 2c displays the time evolution of gel volume ( $V$ ) obtained from the data in Figure 2a. The volume in the figure is reduced by that before stretching ( $V_0$ ). No appreciable volume change occurs in the fast stretching process because  $V/V_0 \approx 1$  at  $t = 0$ . The total increase of volume under constant stretching increases with  $\alpha_x$  because  $V/V_0$  is given by  $\alpha_x^{1-2\mu_\infty}$ . It should be noted that when the imposed strain or stress was removed, the gel completely recovered its original volume before stretching. This shrinking process occurred in the same time scale as the strain-induced swelling.

Figure 3 shows semilog plots of  $\Delta w(t)/\Delta w(\infty)$  and  $\Delta f(t)/\Delta f(\infty)$  versus  $t$  where  $\Delta w(t) = w(0) - w(t)$  and  $\Delta f(t) = f(0) - f(t)$ , and  $\infty$  corresponds to the equilibrium state. For each value of  $\alpha_x$ , all the data points except those corresponding to relatively short times fall on a straight line, the inverse of the slope of which determines the longest characteristic time  $\tau_1$ . A deviation from the linear relation at relatively short times is attributed to the fact that the swelling kinetics is generally expressed by a multi-exponential function with various characteristic times, not by a single-exponential function. This is also theoretically expected (eq 12), and the similar kinetics was well-known in the free swelling of gels.<sup>22</sup> The identical values of  $\tau_1$  with regard to  $w$  and  $f$  at each value of  $\alpha_x$  indicate that the induced swelling and stress reduction proceed simultaneously. The time  $\tau_1$  becomes smaller with increasing  $\alpha_x$  because the stretching process results in a reduction in the gel thickness ( $a$ ), which governs the time required for diffusion. As is seen in the inset of the figure,  $\tau_1$  is proportional to the square of the equilibrium thickness ( $a_\infty$ ) at each  $\alpha_x$ . These results clearly demonstrate that the stress relaxation process is controlled by diffusion, not by viscoelastic effect. The diffusion constant ( $D$ ) is estimated to be  $3.3 \times 10^{-10}$

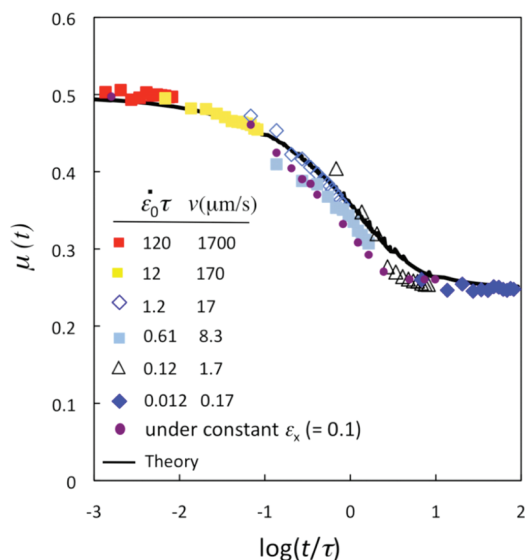


**Figure 5.** Poisson's ratio ( $\mu$ ) as a function of elapsed time ( $t$ ) for the tensile stretching measurements carried out with varying  $v$ . The solid line represents the corresponding theoretical prediction. The  $t$  dependence of  $\mu$  obtained from the measurement under a constant stretch of  $\alpha_x = 1.1$  (Figure 2a) is also shown.

$\text{m}^2/\text{s}$  for  $D \approx a_\infty^2/\tau_1$ , which is of the same order of magnitude as reported values of  $D$  for poly(acrylamide) hydrogels with different concentrations of network and cross-linker.<sup>8,21,23</sup>

**Poisson's Ratio and True Stress during the Stretching Process for Various Crosshead Speeds.** Figure 4 shows the lateral true strain ( $\varepsilon_y$ ) as a function of the true strain ( $\varepsilon_x$ ) imposed during the stretching process for various values of  $v$ . The Poisson's ratio ( $\mu$ ), which is determined by the slope in this curve, varies from 0.5 to  $\sim 0.25$  depending on  $v$ . The product of initial strain rate ( $\dot{\varepsilon}_0 = v/l_0$ ) and the characteristic time of swelling ( $\tau$ ) provides a simple measure of comparison between the characteristic time scales of stretching and swelling. We estimate here the characteristic time of swelling ( $\tau$ ) for an initial thickness ( $a_0$ ), i.e.,  $\tau = a_0^2/D = 4.40 \times 10^3$  s. At the high crosshead speed of  $v_c > 830 \mu\text{m/s}$  ( $\dot{\varepsilon}_0\tau > 61$ ), all data points fall on a straight line with a slope of  $1/2$ . This indicates that during the entire process of stretching, the gel is deformed without volume change; i.e., no strain-induced swelling occurs. A finite stretching-induced swelling is observed at relatively low stretching speed of  $v < 170 \mu\text{m/s}$  ( $\dot{\varepsilon}_0\tau < 12$ ). The value of  $\mu$  decreases with decreasing  $v$ , and  $\mu$  becomes independent of  $v$  at the extremely low stretching speed of  $v < 0.83 \mu\text{m/s}$  ( $\dot{\varepsilon}_0\tau < 0.061$ ). At so low a stretching speed, the strain-induced swelling is equilibrated during the course of the stretching process. The lower limit of  $\mu$  ( $\approx 0.25$ ) is in agreement with the value of  $\mu_\infty$  obtained by the measurements conducted under constant strain (Figure 2a).

The solid lines in the figure correspond to the theoretical  $\varepsilon_y$ – $\varepsilon_x$  relation at various  $\dot{\varepsilon}_0\tau$  obtained from eqs 14–16 using  $\mu_0 = 1/2$  and  $\mu_\infty = 1/4$ . The  $v$  dependence of the  $\varepsilon_y$ – $\varepsilon_x$  relations is satisfactorily described by the theoretical model used. However, for  $\dot{\varepsilon}_0\tau < 1$ , the experimental data tend to become smaller than the theoretical values at relatively high  $\varepsilon_x$ . This is because a significant decrease in gel thickness caused by high  $\varepsilon_x$  accelerates the diffusion. This acceleration effect is not considered in theory; i.e.,  $\tau$  is assumed to be constant during the elongation of the specimen. The  $a$  dependence of  $\tau$ ,  $\tau(a)$ , is a rather difficult

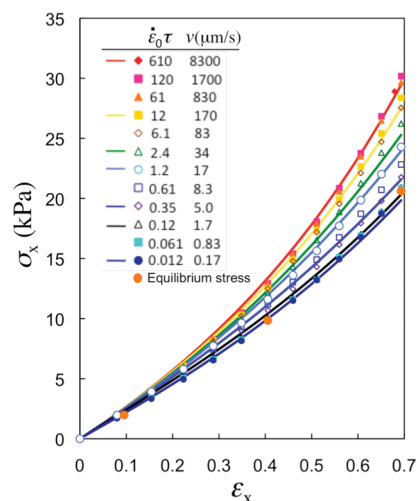


**Figure 6.** Relation between imposed true strain ( $\epsilon_x$ ) and true tensile stress ( $\sigma_x$ ) for a poly(acrylamide) hydrogel undergoing stretching in water over a wide range of crosshead speeds ( $\nu$ ). The solid lines represent theoretical predictions.

theoretical problem because  $a(t)$  also depends on  $\tau$  as shown by eq 15.

Figure 5 shows the time dependence of  $\mu$  for various values of  $\nu$  where  $t$  is reduced by  $\tau$ . The value of  $\mu(t)$  is estimated from the gradient of Figure 4 at the corresponding  $t$ . In the figure,  $\mu(t)$  obtained by the measurement at a constant  $\epsilon_x$  (Figure 2a) is also shown. The data of  $\mu(t)$  obtained at various  $\nu$  form a master curve. Further, the  $\mu(t)$  curve obtained from the measurement at a constant  $\epsilon_x$  is almost identical to the master curve formed by the collection of the data of  $\mu(t)$  at various  $\nu$ . These results indicate that during the stretching process  $\mu$  is simply governed by the time that has elapsed since the specimen starts being elongated. In the short time region of  $t/\tau < 10^{-2}$  where  $t$  is considerably smaller than  $\tau$ ,  $\mu$  is equal to  $\mu_0$  ( $\approx 0.5$ ) independently of time. In the time scale over about 3 orders of magnitude, i.e.,  $10^{-2} < t/\tau < 10^1$ ,  $\mu$  is time-dependent, and  $\mu$  gradually decreases from  $\mu_0$  to  $\mu_\infty$  with increasing  $t$ . The value of  $\mu$  at  $t \approx \tau$  is ca. 0.35. In the long time region of  $t/\tau > 10^1$  where  $t$  is significantly larger than  $\tau$ ,  $\mu$  is  $t$ -independent and equivalent to  $\mu_\infty$  ( $\approx 0.25$ ). It should be noted that the theoretical curve reproduces with sufficient accuracy the experimental master curve of  $\mu(t)$ .

Figure 6 shows  $\sigma$  as a function of  $\epsilon_x$  for various values of  $\nu$ . The  $\nu$  dependence of the stress–strain curve is qualitatively similar to that of the  $\epsilon_x$ – $\epsilon_y$  relation (Figure 4). This behavior indicates that the  $\nu$  dependence of stress originates primarily from the strain-induced swelling. The stress–strain curve at a relatively high  $\nu$  ( $\nu > 830 \mu\text{m/s}$ ;  $\dot{\epsilon}_0\tau > 61$ ) is independent of  $\nu$ . In this regime, the gel behaves as an elastic material without any volume change ( $\mu = 1/2$ ). A considerable reduction is observed in stress at a relatively low elongation speed of  $\nu < 170 \mu\text{m/s}$  ( $\dot{\epsilon}_0\tau < 12$ ) where a finite stretching-induced swelling is observed. The stress–strain curve corresponding to an extremely low elongation speed of  $\nu < 0.83 \mu\text{m/s}$  ( $\dot{\epsilon}_0\tau < 0.061$ ) coincides with the equilibrium curve where the strain-induced swelling saturates throughout the stretching process. In fact, the equilibrium stresses estimated under a constant strain (Figure 2b) fall on the stress–strain curves in the low  $\nu$  regime of  $\nu < 0.83 \mu\text{m/s}$ . These results show that the  $\nu$

dependence of the stress–strain relations is governed by the  $\nu$  dependence of strain-induced swelling. The viscoelastic effect stemming from the structural defects such as dangling chains can be neglected here.

The  $\sigma$ – $\epsilon_x$  relation for relatively high values of  $\nu$  when the specimen's volume does not change during its deformation is described by eq 9 (eq 7 with  $\mu = 1/2$ ), i.e., the prediction of the classical rubber elasticity theory. It has been empirically known that the uniaxial stress–strain behavior of conventional cross-linked rubbers and chemical gels at a fully swollen state obeys eq 9 almost independently of types of polymer and solvent.<sup>17</sup> As the data for previous studies were collected through experiments conducted in air, they correspond to cases where the specimen's volume does not change during its deformation. The  $\sigma$ – $\epsilon_x$  relation in the low  $\nu$  limit is successfully approximated by eq 8 (eq 7 with  $\mu = 1/4$ ). These results show that the theory accounts for the effects of the induced swelling on stress in the long time limit. Furthermore, the  $\nu$  dependence of the  $\sigma$ – $\epsilon_x$  relations is satisfactorily reproduced by the theoretical model. The theoretical stress–strain curves at various  $\nu$  were calculated using eq 7 with the theoretical value of  $\mu$  at the corresponding  $t$  and  $G = 8.5 \text{ kPa}$ . The diffusion acceleration caused by the thinning of the specimen, which is not considered in the theoretical model, does not appreciably affect the stress, although it becomes significant for a lateral strain at  $\dot{\epsilon}_0\tau < 1$  (Figure 4). Its effect on the stress may be too small to detect because the total stress difference between high and low  $\dot{\epsilon}_0$  values is as large as 30%.

A finite strain-rate dependence of stress was observed for the 1 mm thick gels at considerably slow stretching speeds ( $\nu < 0.1 \text{ mm/s}$ ). It should be noted that the finite strain-rate dependence becomes pronounced at easily attainable stretching speeds for the gels with small dimensions such as microfabricated gels and fiber gels because the corresponding  $\tau$  is considerably small ( $\tau \propto a^2$ ).

## SUMMARY

A series of tensile stretching experiments covering a wide range of strain rates and including an extremely slow stretching speed of  $0.17 \mu\text{m/s}$  revealed the whole aspects of the  $\nu$ -dependent  $\mu$  and  $\sigma$  for the fully swollen gels greatly stretched in solvents. In the case of a relatively high stretching speed, where the time scale of stretching ( $\dot{\epsilon}_0^{-1}$ ) is considerably shorter than the characteristic time of swelling ( $\tau$ ), no strain-induced swelling occurs, and the gel behaves as an elastic material with  $\mu = 1/2$ . When the stretching speed is so slow that  $\dot{\epsilon}_0^{-1}$  is comparable to  $\tau$ ,  $\mu$  and  $\sigma$  considerably depend on  $\dot{\epsilon}_0$  due to the finite degree of strain-induced swelling observed during stretching. For these  $\dot{\epsilon}_0$  values,  $\mu$  and  $\sigma$  decrease as the stretching speed decreases. At extremely low stretching speeds satisfying the relation  $\dot{\epsilon}_0^{-1} \gg \tau$ , the gel exhibits the equilibrium value of  $\mu$  ( $\approx 0.25$ ) and  $\sigma$  independently of the value of  $\dot{\epsilon}_0$  due to the equilibration of the induced swelling throughout the stretching process. The  $\nu$  dependence of  $\mu$  and stress–strain relation observed was satisfactorily described by a theoretical model that was developed based on existing models for the swelling behavior observed after the application of a small step strain on the basis of the Boltzmann superposition principle. The finite strain-rate-dependent Poisson's ratio and stress become pronounced at easily attainable deformation rates for microfabricated gels and fiber gels with relatively short characteristic time for swelling.

## AUTHOR INFORMATION

### Corresponding Author

\*E-mail: urayama@rheogate.polym.kyoto-u.ac.jp.

## ACKNOWLEDGMENT

This work was partly supported by a Grant-in-Aid for Scientific Research on Priority Area "Soft Matter Physics" (No. 21015014) from the Ministry of Education, Culture, Sports, Science and Technology (MEXT), Japan.

## REFERENCES

- (1) *Gels Handbook*; Academic Press: San Diego, 2000.
- (2) Hecht, A. M.; Geissler, E. *J. Chem. Phys.* **1980**, *73*, 4077–4080.
- (3) Chiarelli, P.; Bassar, P. J.; Derossi, D.; Goldstein, S. *Biorheology* **1992**, *29*, 383–398.
- (4) Takigawa, T.; Urayama, K.; Morino, Y.; Masuda, T. *Polym. J.* **1993**, *25*, 929–937.
- (5) Milimouk, I.; Hecht, A. M.; Beysens, D.; Geissler, E. *Polymer* **2001**, *42*, 487–494.
- (6) Vervoort, S.; Patlazhan, S.; Weyts, J.; Budtova, T. *Polymer* **2005**, *46*, 121–127.
- (7) Zanina, A.; Budtova, T. *Macromolecules* **2002**, *35*, 1973–1975.
- (8) Urayama, K.; Okada, S.; Nosaka, S.; Watanabe, H.; Takigawa, T. *J. Chem. Phys.* **2005**, *122*, 024906.
- (9) Nosaka, S.; Urayama, K.; Takigawa, T. *Polym. J.* **2005**, *37*, 694–699.
- (10) Murata, N.; Konda, A.; Urayama, K.; Takigawa, T.; Kidowaki, M.; Ito, K. *Macromolecules* **2009**, *42*, 8485–8491.
- (11) Urayama, K.; Taoka, Y.; Nakamura, K.; Takigawa, T. *Polymer* **2008**, *49*, 3295–3300.
- (12) Flory, P. J.; Rehner, J. *J. Chem. Phys.* **1943**, *11*, 521–526.
- (13) Flory, P. J. *Principles of Polymer Chemistry*; Cornell University Press: Ithaca, NY, 1953.
- (14) Daoud, M.; Degennes, P. G. *J. Phys. (Paris)* **1977**, *38*, 85–93.
- (15) Alexander, S.; Rabin, Y. *J. Phys.: Condens. Matter* **1990**, *2*, Sa313–Sa315.
- (16) Geissler, E.; Hecht, A. M.; Horkay, F.; Zrinyi, M. *Macromolecules* **1988**, *21*, 2594–2599.
- (17) Treloar, L. R. G. *The Physics of Rubber Elasticity*, 3rd ed.; Clarendon Press: Oxford, 1975.
- (18) Yamaue, T.; Doi, M. *J. Chem. Phys.* **2005**, *122*, 084703.
- (19) Doi, M. *J. Phys. Soc. Jpn.* **2009**, *78*, 052001.
- (20) Urayama, K.; Murata, N.; Nosaka, S.; Kojima, M.; Takigawa, T. *Colloid Polym. Sci.* **2009**, *136*, 107–112.
- (21) Tanaka, T.; Fillmore, D. J. *J. Chem. Phys.* **1979**, *70*, 1214–1218.
- (22) Takigawa, T.; Urayama, K.; Masuda, T. *Polym. J.* **1994**, *26*, 225–227.
- (23) Li, Y.; Tanaka, Y. *J. Chem. Phys.* **1990**, *92*, 1365–1371.